



# Maturing Space-Based Precision Metrology with Quantum Gas Studies Aboard the ISS

Jason Williams

*Quantum Sciences and Technology Group*

*Jet Propulsion Laboratory, California Institute of Technology, Pasadena, CA, USA.*

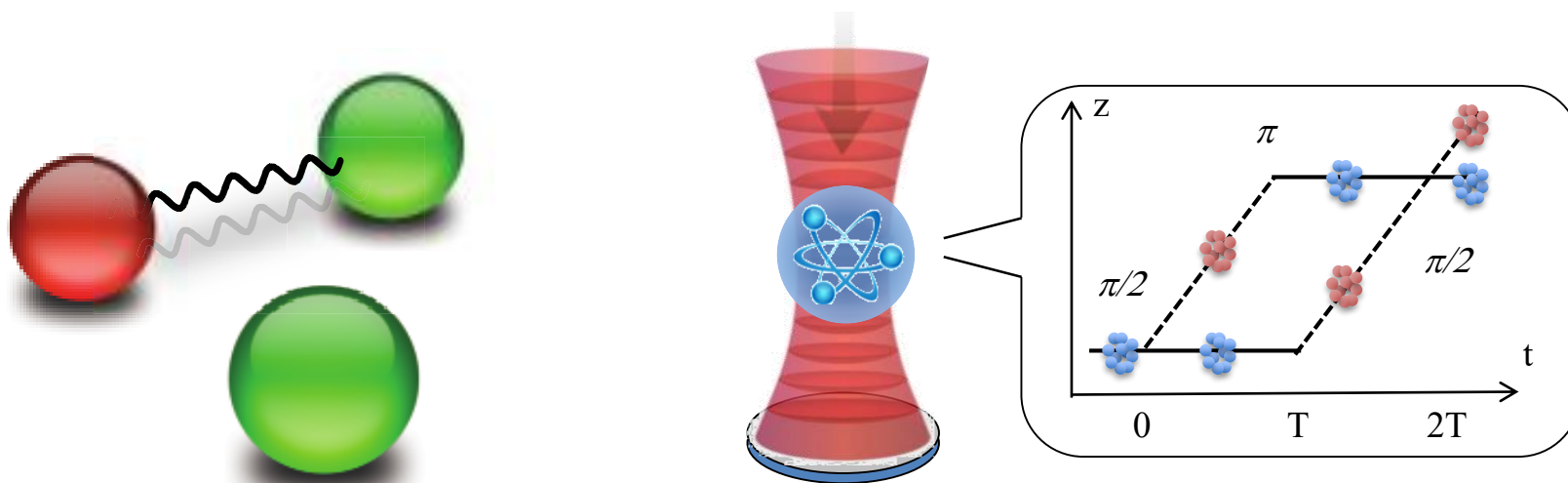
## Introduction

- Atom interferometers (AI) as inertial sensors and applications in space.

## Pathfinder studies with dual-species AI on the ISS

- Unprecedented atom-photon coherence time in CAL.
- Interferometric detection of relevant ISS vibration and rotation environment.
- Resonant molecular (Feshbach) physics in the ultracold regime for controlling systematics.
- Follow on studies and wish-list for BEcCAL.

## Design and characterization studies of the CAL AI ORU





Wuhan 10m drop tower

PRL 115, 013004 (2015)

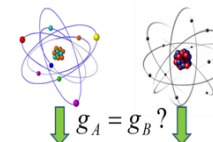
PHYSICAL REVIEW LETTERS

week ending  
3 JULY 2015

## Test of Equivalence Principle at $10^{-8}$ Level by a Dual-Species Double-Diffraction Raman Atom Interferometer

Lin Zhou,<sup>1,2</sup> Shitong Long,<sup>1,2,3</sup> Biao Tang,<sup>1,2</sup> Xi Chen,<sup>1,2</sup> Fen Gao,<sup>1,2</sup> Wencui Peng,<sup>1,2</sup> Weitao Duan,<sup>1,2,3</sup> Jiaqi Zhong,<sup>1,2</sup>  
Zongyuan Xiong,<sup>1,2</sup> Jin Wang,<sup>1,2,\*</sup> Yuanzhong Zhang,<sup>4</sup> and Mingsheng Zhan<sup>1,2,†</sup>

Dual-isotope  $^{87}\text{Rb}$ - $^{85}\text{Rb}$  AI test of the  
Weak Equivalence Principle to  $3 \times 10^{-8}$ .



PRL 113, 023005 (2014)

PHYSICAL REVIEW LETTERS

week ending  
11 JULY 2014

## Test of Einstein Equivalence Principle for 0-Spin and Half-Integer-Spin Atoms: Search for Spin-Gravity Coupling Effects

M. G. Tarallo,<sup>\*</sup> T. Mazzoni, N. Poli, D. V. Sutyurin, X. Zhang,<sup>†</sup> and G. M. Tino<sup>‡</sup>  
*Dipartimento di Fisica e Astronomia and LENS—Università di Firenze, INFN—Sezione di Firenze,  
Via Sansone 1, 50019 Sesto Fiorentino, Italy*  
(Received 24 February 2014; published 8 July 2014)

Dual-isotope  $^{88}\text{Sr}$ - $^{87}\text{Sr}$  AI test of the  
Weak Equivalence Principle to  $\sim 10^{-7}$ .

PRL 112, 203002 (2014)

PHYSICAL REVIEW LETTERS

week ending  
23 MAY 2014

## Quantum Test of the Universality of Free Fall

D. Schlippert,<sup>1</sup> J. Hartwig,<sup>1</sup> H. Albers,<sup>1</sup> L. L. Richardson,<sup>1</sup> C. Schubert,<sup>1</sup> A. Roura,<sup>2</sup> W. P. Schleich,<sup>2,3</sup>  
W. Ertmer,<sup>1</sup> and E. M. Rasel<sup>1\*</sup>

<sup>1</sup>*Institut für Quantenoptik and Centre for Quantum Engineering and Space-Time Research (QUEST),  
Leibniz Universität Hannover, Welfengarten 1, D-30167 Hannover, Germany*

<sup>2</sup>*Institut für Quantenphysik and Center for Integrated Quantum Science and Technology (IQST),  
Universität Ulm, Albert-Einstein-Allee 11, D-89081 Ulm, Germany*

<sup>3</sup>*Texas A&M University Institute for Advanced Study (TIAS), Institute for Quantum Science and Engineering (IQSE)  
and Department of Physics and Astronomy, Texas A&M University, College Station, Texas 77843-4242, USA*  
(Received 1 April 2014; published 22 May 2014)

Dual-species  $^{87}\text{Rb}$ - $^{39}\text{K}$  AI test of the  
Weak Equivalence Principle to  $5 \times 10^{-7}$ .



PRL **103**, 050402 (2009)

PHYSICAL REVIEW LETTERS

week ending  
31 JULY 2009

## Noise-Immune Conjugate Large-Area Atom Interferometers

Sheng-wei Chiow,<sup>1</sup> Sven Herrmann,<sup>1</sup> Steven Chu,<sup>1,2,3</sup> and Holger Müller<sup>1,2,3,\*</sup>

<sup>1</sup>Physics Department, Stanford University, 382 Via Pueblo Mall, Stanford, California 94305, USA

<sup>2</sup>Department of Physics, University of California, 366 Le Conte Hall, Berkeley, California 94720-7300, USA

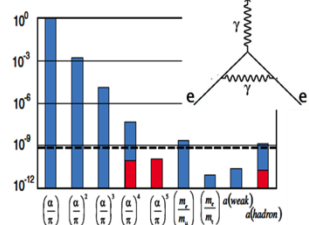
<sup>3</sup>Lawrence Berkeley National Laboratory, One Cyclotron Road, Berkeley, California 94720, USA

(Received 13 January 2009; published 28 July 2009)

$$\alpha = [(2R_\infty/c)(M/m_e)(h/M)]^{1/2}$$

measured to 3.4 ppb

Fine structure constant, QED



Quantum mass standard



## Atom-interferometry constraints on dark energy

SCIENCE sciencemag.org  
21 AUGUST 2015 • VOL 349 ISSUE 6250

P. Hamilton,<sup>1,\*</sup> M. Jaffe,<sup>1</sup> P. Haslinger,<sup>1</sup> Q. Simmons,<sup>1</sup> H. Müller,<sup>1,2,†</sup> J. Khoury<sup>3</sup>

If dark energy, which drives the accelerated expansion of the universe, consists of a light scalar field, it might be detectable as a “fifth force” between normal-matter objects, in potential conflict with precision tests of gravity. Chameleon fields and other theories with screening mechanisms, however, can evade these tests by suppressing the forces in regions of high density, such as the laboratory. Using a cesium matter-wave interferometer near a spherical mass in an ultrahigh-vacuum chamber, we reduced the screening mechanism by probing the field with individual atoms rather than with bulk matter. We thereby constrained a wide class of dark energy theories, including a range of chameleon and other theories that reproduce the observed cosmic acceleration.

NASA Fundamental Physics Workshop, La Jolla, CA

PHYSICAL REVIEW A **91**, 033629 (2015)

## Testing gravity with cold-atom interferometers

G. W. Biedermann,<sup>\*</sup> X. Wu, L. Deslauriers, S. Roy, C. Mahadeswaraswamy, and M. A. Kasevich<sup>†</sup>

Physics Department, Stanford University, Stanford, California 94305, USA

(Received 1 December 2014; published 24 March 2015)

For a Yukawa force, the acceleration is given by

$$a_i = \frac{Gm}{r_i^2} [1 + \alpha e^{-r_i/\lambda} (1 + r_i/\lambda)].$$

Constraint on Yukawa-type fifth force at  $8 \times 10^{-3}$  near “poorly known” length scale of 10cm.

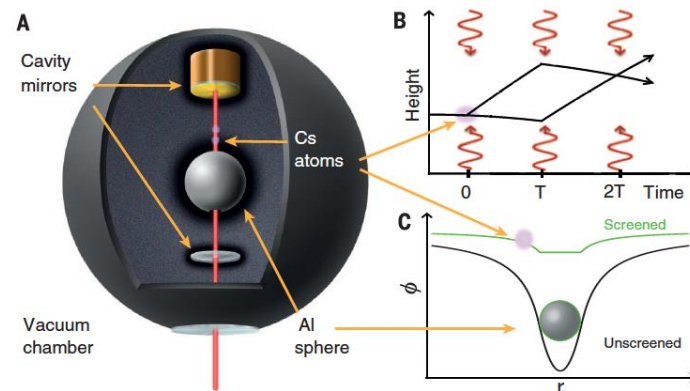
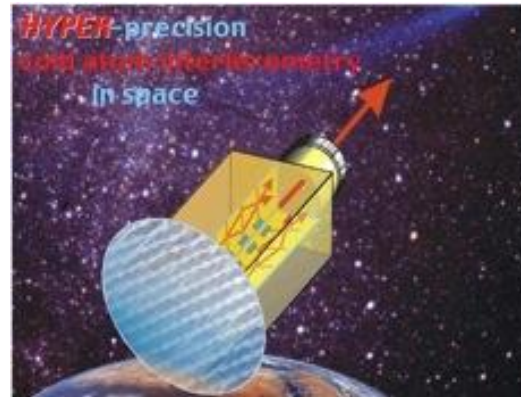


**Fig. 1. Screened fields in our experiment.** (A) The vacuum chamber (radius, 5 cm; pressure,  $\sim 6 \times 10^{-10}$  Torr; mostly hydrogen) holds a pair of mirrors forming a Fabry-Perot cavity and the aluminum source sphere. Laser beams pass through a 1.5-mm-radius hole in the sphere (radius of the sphere, 9.5 mm). A Mach-Zehnder interferometer is formed using cold cesium atoms from a magneto-optical trap at an effective distance of 8.8 mm from the sphere surface (not shown). (B) Photons in three flashes of laser radiation that are resonant in the cavity impart momentum to the atoms, directing each atomic matter wave onto two paths. (C) The potential generated by a macroscopic sphere as a function of distance from the sphere's center.

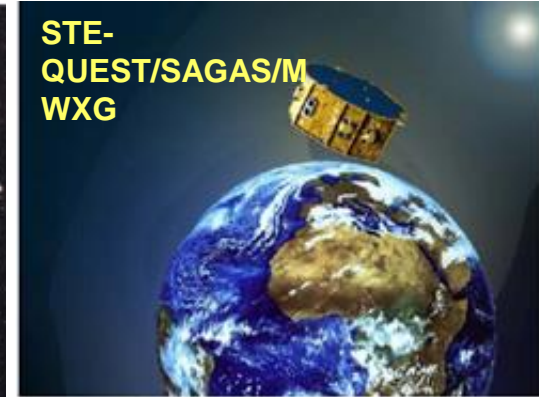
April 09, 2018

## Precision inertial measurements for advancement of science

- Frame-dragging test of the General Relativity Theory
- Test of Einstein's Equivalence Principle with differential acceleration measurements of two atomic species
- Gravitational wave detection
- Spin-gravity coupling with quantized angular momentum states
- Signatures of dark matter and dark energy

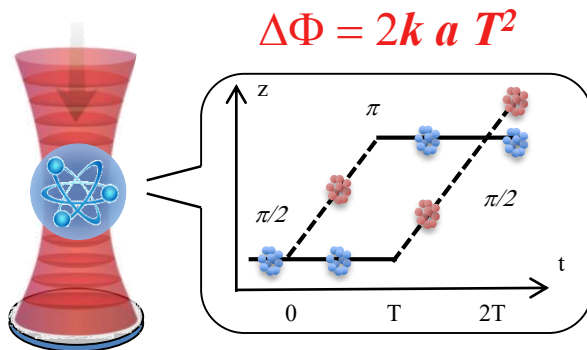


Precision measurements of Lense-Thirring effect



Space-Time Explorer and Quantum Equivalence Principle Space Test

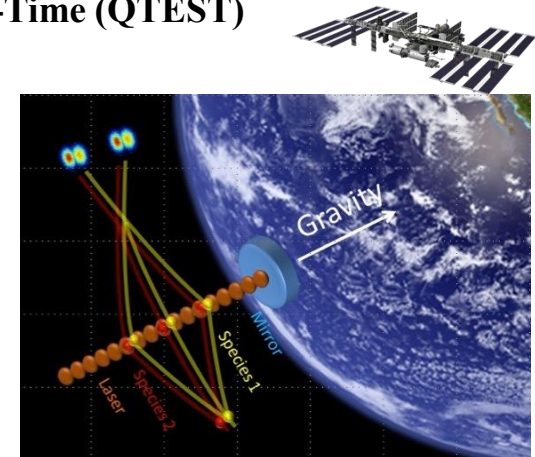
## Light-Pulse Atom Interferometer:



## Quantum Test of the Equivalence Principle and Space-Time (QTEST)

State of the art dual-species atom interferometer as a multi-user facility onboard the ISS for:

- Test the Weak Equivalence Principle (WEP) to below  $10^{-15}$  with *quantum* test masses.
- Measure the fine structure constant ( $\alpha$ ) to  $10^{-12}$  precision for most precise test of QED.
- Most precise primary mass standard in the proposed SI.



Gravity effects on two different atomic species ( $^{87}\text{Rb}$  and  $^{85}\text{Rb}$ ) are compared in space.

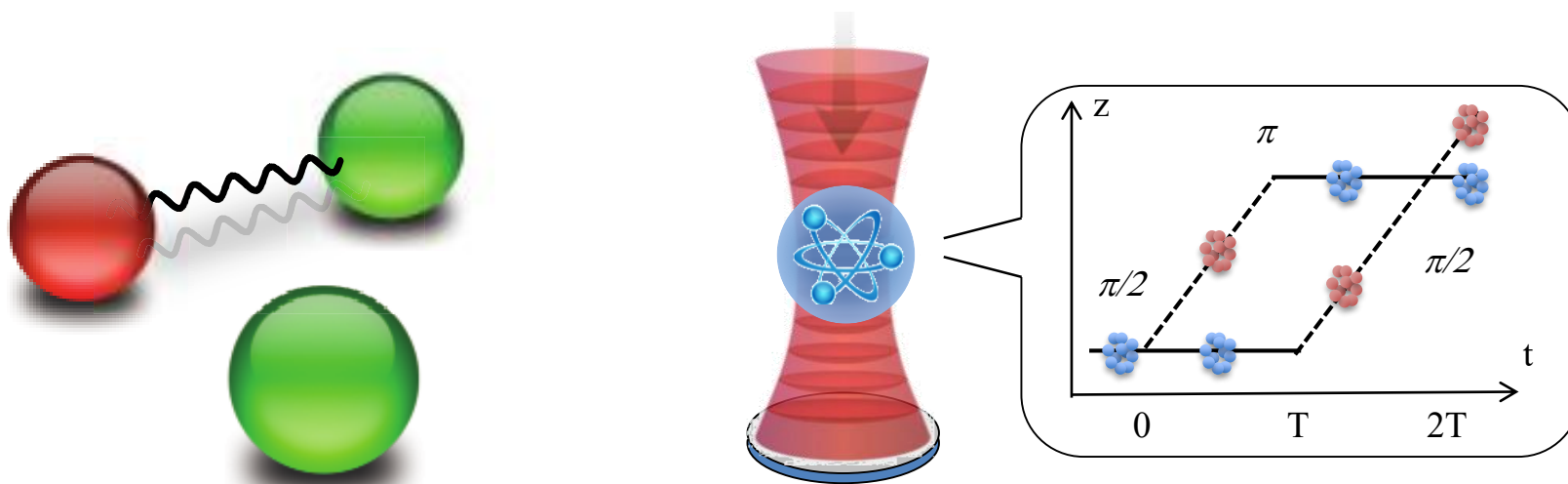
## Introduction

- Atom interferometers (AI) as inertial sensors and applications in space.

## Pathfinder studies with dual-species AI on the ISS

- Unprecedented atom-photon coherence time in CAL.
- Interferometric detection of relevant ISS vibration and rotation environment.
- **Resonant molecular (Feshbach) physics in the ultracold regime for controlling systematics.**
- Follow on studies and wish-list for BEcCAL.

## Strontium testbed at JPL to mature precision sensors/clocks for ground and space



# Challenges for Long-T Interferometers

**Known sources that can limit the ultimate accuracy of high-precision WEP tests include: vibrations, rotations, magnetic fields, differential center-of-mass position and velocity, ...**

Assuming  $\delta v = 1 \mu\text{m/s}$ ,  $\delta r = 1 \mu\text{m}$ ,  $\delta \Omega = 10^{-3} \Omega_{\text{ISS}}$ ,  $a = 100 a_0$ ,  $n_0 = 2 \times 10^8/\text{cm}^3$ ,  $2T = 20\text{s}$

## Gravity gradient shifts

- Test masses traveling different classical paths ( $\delta r$ ,  $\delta v$ ) experience different gravitational potentials.

$$k_{\text{eff}} g_{zz} (dz + dvT) T^2 = 3.0 \times 10^{-12} g$$

## Rotations (centrifugal and Coriolis)

- Reduces signal contrast and systematics from different velocities.

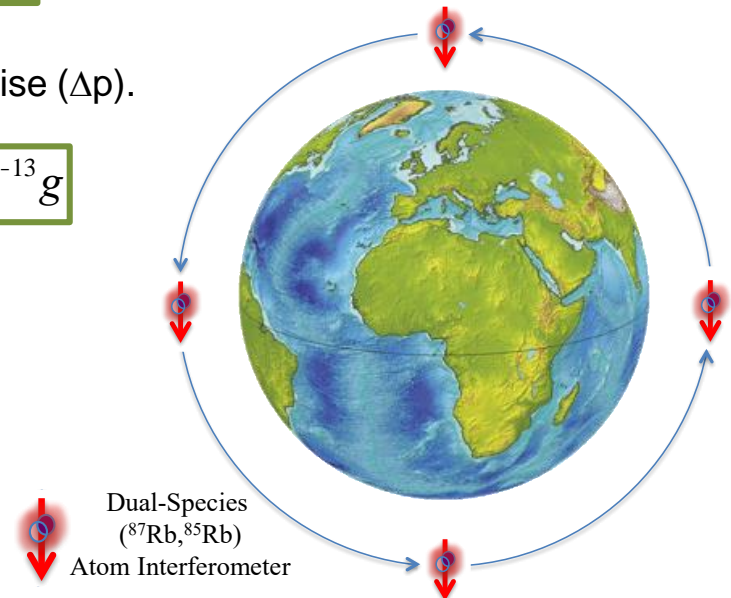
$$-2k_{\text{eff}} dv_z dN_y T^2 = 2.6 \times 10^{-13} g$$

## Mean-field shift:

- Scales with interaction strength and beam-splitter efficiency/noise ( $\Delta p$ ).
- Fundamental density limit.

$$(4\rho \hbar a_{ij} / m) n_{j0} DpT = 3.8 \times 10^{-13} g$$

Orders of magnitude enhanced cloud overlap necessary for WEP tests to  $10^{-15} g$ .





# Challenges for Long-T Interferometers

Known sources that can limit the ultimate accuracy of high-precision WEP tests include: vibrations, rotations, magnetic fields, differential center-of-mass position and velocity, ...

Assuming  $\delta v = 1 \mu\text{m/s}$ ,  $\delta r = 1 \mu\text{m}$ ,  $\delta \Omega = 10^{-3} \Omega_{\text{ISS}}$ ,  $a = 100 a_0$ ,  $n_0 = 2 \times 10^8/\text{cm}^3$ ,  $2T = 20\text{s}$

## Gravity gradient shifts

- Test masses traveling different classical paths ( $\delta r$ ,  $\delta v$ ) experience different gravitational potentials.

$$k_{\text{eff}} g_{zz} (dz + dvT) T^2 = 3.0 \times 10^{-12} g$$

## Rotations (centrifugal and Coriolis)

- Reduces signal contrast and systematics from different velocities.

$$-2k_{\text{eff}} dv_z dN_y T^2 = 2.6 \times 10^{-13} g$$

Orders of magnitude enhanced cloud overlap necessary for WEP tests to  $10^{-15} g$ .

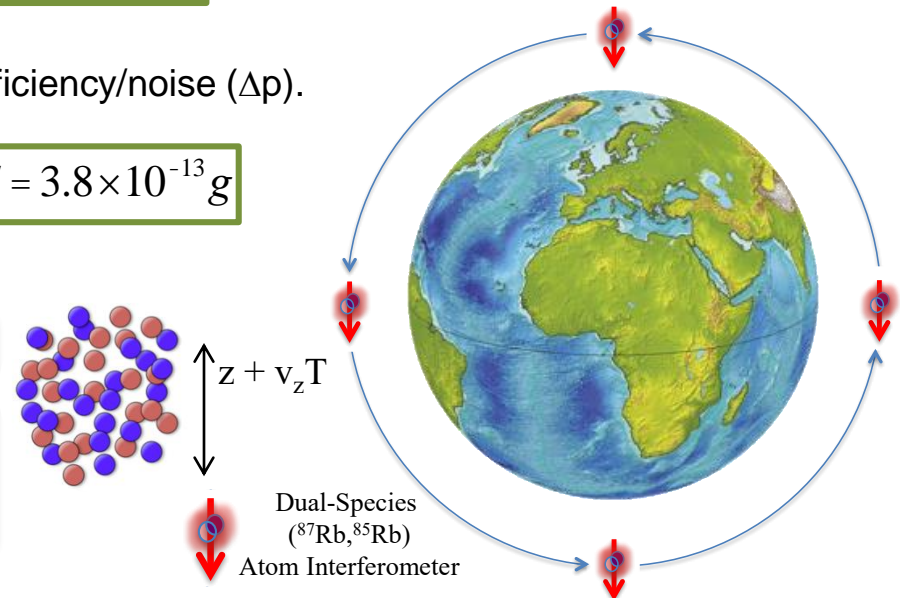
## Mean-field shift:

- Scales with interaction strength and beam-splitter efficiency/noise ( $\Delta p$ ).
- Fundamental density limit.

$$(4p\hbar a_{ij} / m) n_{j0} DpT = 3.8 \times 10^{-13} g$$

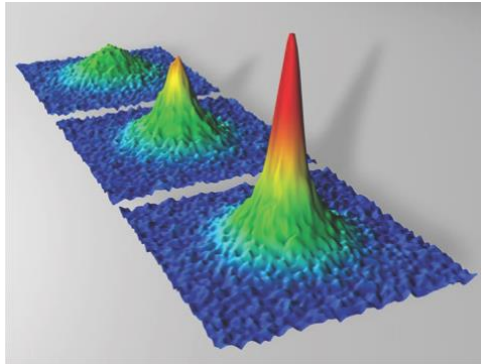
## Contrast loss from $\Delta\Phi$ across the cloud\*:

	Phase Term	$\Delta\Phi$ at $T = 0.5\text{s}$	$T = 10\text{s}$	Notes
1	$k_{\text{eff}} g T^2$	$3.9 \times 10^7$	$1.6 \times 10^{10}$	Gravitational
2	$2k_{\text{eff}} \cdot (\Omega \times \mathbf{v}) T^2$	0.9	370	Coriolis
3	$k_{\text{eff}} \gamma_{zz} (z + v_z T) T^2$	.0005	4.2	Gravity Gradient
4	$(4\pi\hbar a/m) n_0 T$	.03	0.6	Mean Field Shift

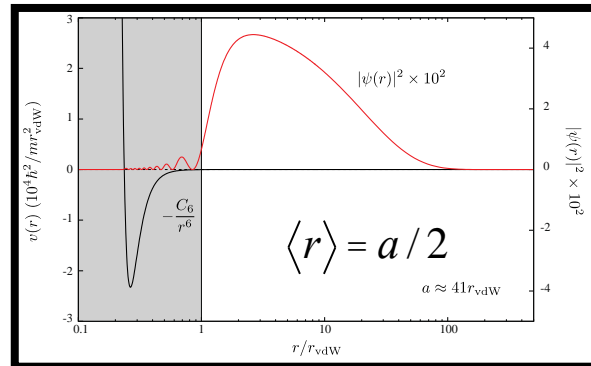




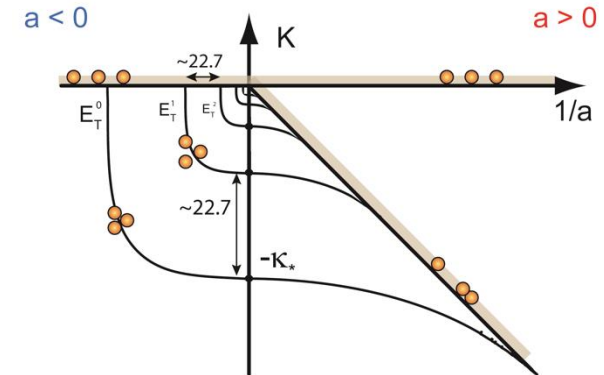
## Fermi Gases: BEC-BCS



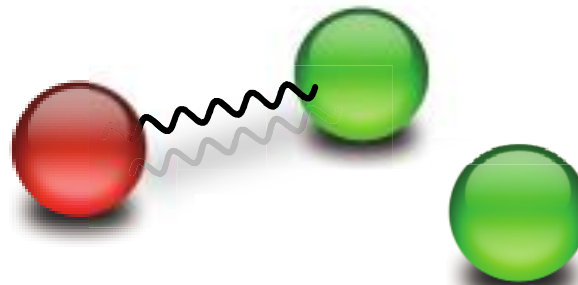
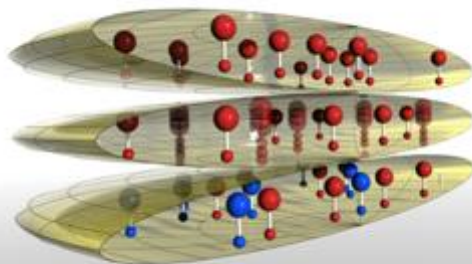
## Halo Molecules



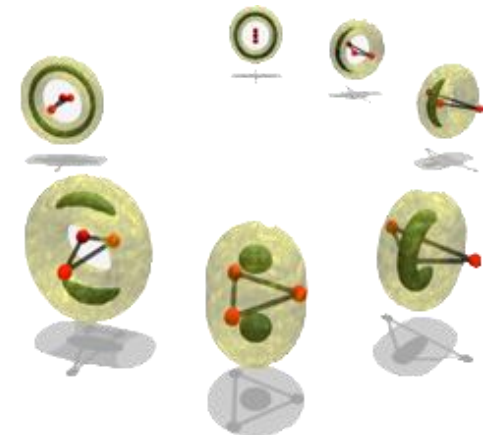
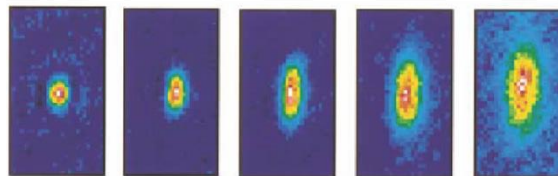
## Universal Few-Body Physics



## Dipolar molecules



## Controlled Interactions and Strongly Correlated Physics

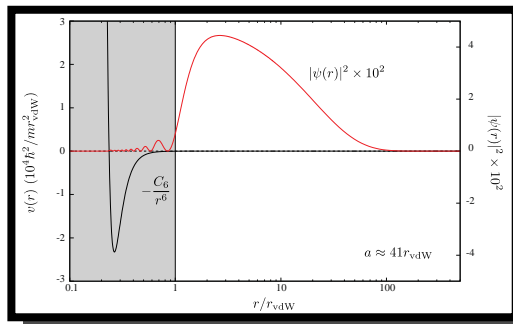


Atom	ch.	$\ell$	$\ell_c$	$B_0$ (G)	$\Delta$ (G)	$a_{bg}/a_0$	$\delta\mu/\mu_B$	$s_{res}$	$r_{bg}$	$\zeta$	Reference
$^{39}\text{K}$	aa	s	s	402.4	-52	-29	1.5	2.1	-0.47	0.49	D'Errico <i>et al.</i> , 2007
$^{40}\text{K}$	bb	p	p	198.4	na	na	0.134	na	na	na	Regal <i>et al.</i> , 2003b; Ticknor <i>et al.</i> , 2004 <sup>a</sup>
	bb	p	p	198.8	na	na	0.134	na	na	na	Regal <i>et al.</i> , 2003b; Ticknor <i>et al.</i> , 2004 <sup>a</sup>
	ab	s	s	202.1	8.0	174	1.68	2.2	2.8	3.1	Regal <i>et al.</i> , 2004 <sup>a</sup>
	ac	s	s	224.2	9.7	174	1.68	2.7	2.8	3.8	Regal and Jin, 2003 <sup>a</sup>
$^{85}\text{Rb}$	ee	s	s	155.04	10.7	-443	-2.33	28	-5.6	80	Claussen <i>et al.</i> , 2003
$^{87}\text{Rb}$	aa	s	s	1007.4	0.21	100	2.79	0.13	1.27	0.08	Volz <i>et al.</i> , 2003; Dürr, Volz, and Rempe, 2004 <sup>a</sup>
	aa	s	s	911.7	0.0013	100	2.71	0.001	1.27	0.0006	Marte <i>et al.</i> , 2002 <sup>a</sup>
	aa	s	s	685.4	0.006	100	1.34	0.006	1.27	0.004	Marte <i>et al.</i> , 2002; Dürr, Volz, and Rempe, 2004 <sup>a</sup>
	aa	s	s	406.2	0.0004	100	2.01	0.0002	1.27	0.0001	Marte <i>et al.</i> , 2002 <sup>a</sup>
	ae	s	s	9.13	0.015	99.8	2.00	0.008	1.27	0.005	Widera <i>et al.</i> , 2004
$^{39}\text{K } ^{87}\text{Rb}$	aa	s	s	317.9	7.6	34	2.0	0.74	0.50	0.18	Simoni <i>et al.</i> , 2008
$^{40}\text{K } ^{87}\text{Rb}$	aa	s	s	546.9	-3.10	-189	2.30	1.96	-2.75	2.70	Pashov <i>et al.</i> , 2007; Simoni <i>et al.</i> , 2008
$^{41}\text{K } ^{87}\text{Rb}$	aa	s	s	39	37	284	1.65	25.8	4.11	53.0	Simoni <i>et al.</i> , 2008; Thalhammer <i>et al.</i> , 2008
$^{41}\text{K } ^{87}\text{Rb}$	aa	s	s	79	1.2	284	1.59	0.81	4.11	1.66	Simoni <i>et al.</i> , 2008; Thalhammer <i>et al.</i> , 2008
$^{85}\text{Rb } ^{87}\text{Rb}$	ec	s	s	265.4	5.8	213					Papp and Wieman, 2006
$^{85}\text{Rb } ^{87}\text{Rb}$	ec	s	s	372	1	213					Papp and Wieman, 2006

C. Chin *et al.*, “Feshbach resonances in ultracold gases”, Rev. Mod. Phys. **82**, 1225 (2010)

## Microgravity provides a unique regime for Feshbach Physics

- Unearthly low energy scales.
- No gravitational sag.
- Extended timescales for few-body physics and loss.



Dimer Size:  $\langle r \rangle = a / 2$

Binding Energy:  $E_D \approx \frac{-\hbar^2}{ma^2}$

## Enhanced association and dissociation of heteronuclear Feshbach molecules in a microgravity environment

J. P. D’Incao,<sup>1,2</sup> M. Krutzik,<sup>3,4</sup> E. Elliott,<sup>4</sup> and J. R. Williams<sup>4</sup>

<sup>1</sup>*JILA, University of Colorado and NIST, Boulder, Colorado, USA*

<sup>2</sup>*Department of Physics, University of Colorado, Boulder, Colorado, USA*

<sup>3</sup>*Humboldt-Universität zu Berlin, Institut für Physik, Berlin, Germany*

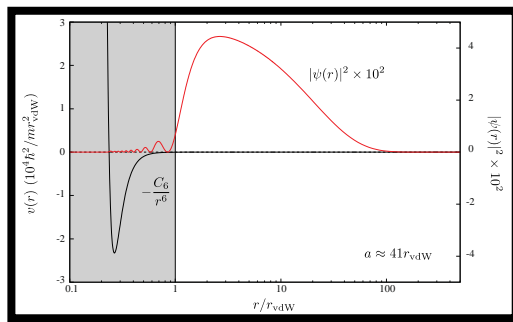
<sup>4</sup>*Jet Propulsion Laboratory, California Institute of Technology, CA, USA*

We study the association and dissociation dynamics of weakly bound heteronuclear Feshbach molecules using transverse RF-fields for expected parameters accessible through the microgravity environment of NASA’s Cold Atom Laboratory (CAL) aboard the International Space Station, including sub nanoKelvin temperatures and atomic densities as low as  $10^8/\text{cm}^3$ . We show that under such conditions, thermal and loss effects can be greatly suppressed resulting in high efficiency in both association and dissociation of Feshbach molecules with mean size exceeding  $10^4 a_0$ , and allowing for the coherence in atom-molecule transitions to be clearly observable. Our theoretical model for heteronuclear mixtures includes thermal, loss, and density effects in a simple and conceptually clear manner. We derive the temperature, density and scattering length regimes of  $^{41}\text{K}$ - $^{87}\text{Rb}$  that allow optimal association/dissociation efficiency with minimal heating and loss to guide upcoming experiments with ultracold atomic gases in space.

PACS numbers: 34.50.-s, 34.50.Cx, 67.85.-d, 67.85.-d

## Microgravity provides a unique regime for Feshbach Physics

- Unearthly low energy scales.
- No gravitational sag.
- Extended timescales for few-body physics and loss.



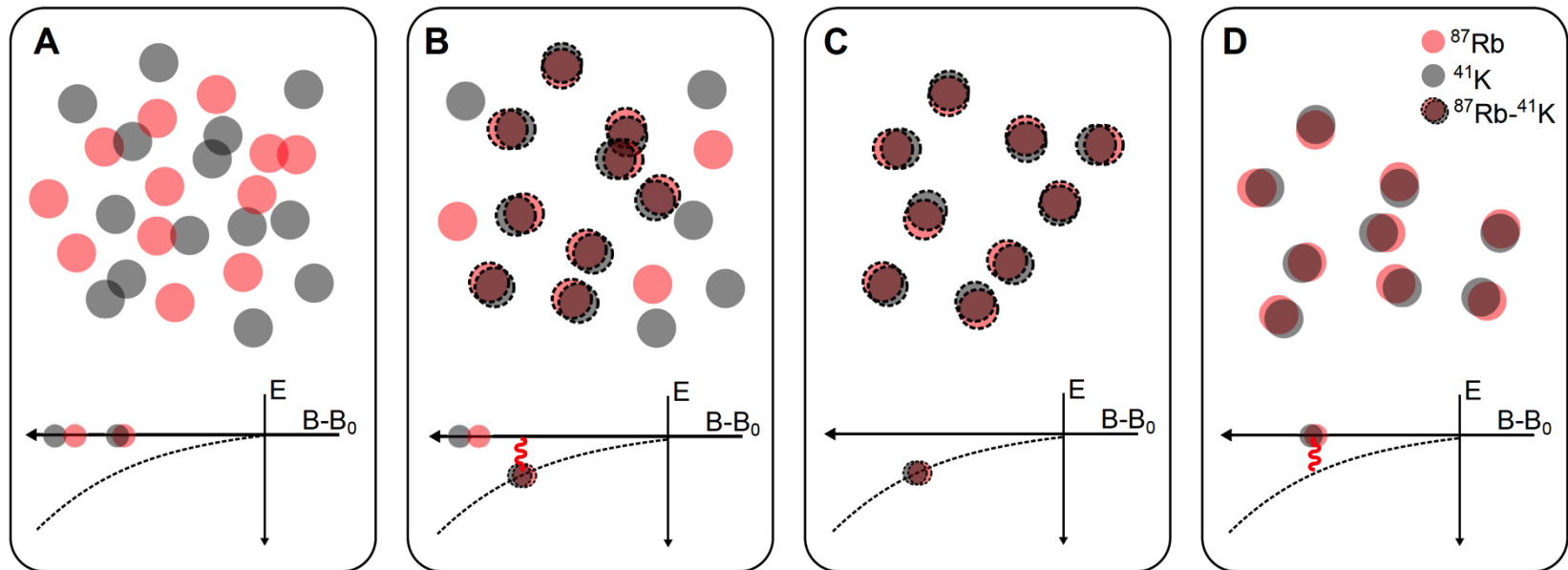
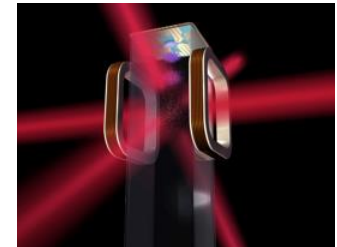
Dimer Size:  $\langle r \rangle = a / 2$

Binding Energy:  $E_D \approx \frac{-\hbar^2}{ma^2}$

#1:

## Low-energy Feshbach physics to prepare highly-overlapped dual-species atomic gases in microgravity

- Negate systematics scaling with  $\delta r$  and  $\delta v$ .
- Molecular state-control at  $k_B \cdot 1$  nK.



- (A) Start with  $^{41}\text{K}$ - $^{87}\text{Rb}$  dual species gases co-trapped and cooled to  $\sim 1$  nK.
- (B + C) Heteronuclear Feshbach molecule formation (RF) and filtering out free atoms
- (D) Molecular dissociation **w/ Fourier-limited heating and negligible loss.**



## Preliminary Error Budget for $^{87}\text{Rb}$ and $^{41}\text{K}$ CM overlap

	Systematic	CM position	CM velocity	Comments
1	1 <sup>st</sup> Order Zeeman	0.17nm	34nm/s	Mitigated by dissociating $^{41}\text{K}$ and $^{87}\text{Rb}$ to the clock states.
2	2 <sup>nd</sup> Order Zeeman	< 0.1nm	2nm/s	Independent of B-field magnitude by field-direction modulation.
3	RF Photon	< 5pm	< 0.5nm/s	Recoil from 35 MHz RF pulse at dissociation.
4	Vibrations	< 4nm		Camera movement over 1 ms assuming $S(g) < 3 \times 10^{-7} g^2 / Hz$ .
5	Gravity	< 50pm		Assuming 10 $\mu\text{g}$ residual acceleration and 1 ms imaging delay between species.
6	Imaging Light	< 1pm		Off-resonant scattering of $^{41}\text{K}$ atoms during imaging pulse for $^{87}\text{Rb}$ .
	<b>Total</b>	<b>&lt; 5 nm</b>	<b>&lt; 3 nm/s</b>	

Assuming  $B = 1$  Gauss and  $\Delta B = 10$  mGauss/cm, detection 10ms after dissociation, RF spectroscopy and Stern-Gerlach separation to characterize fields to a part in  $10^3$ .

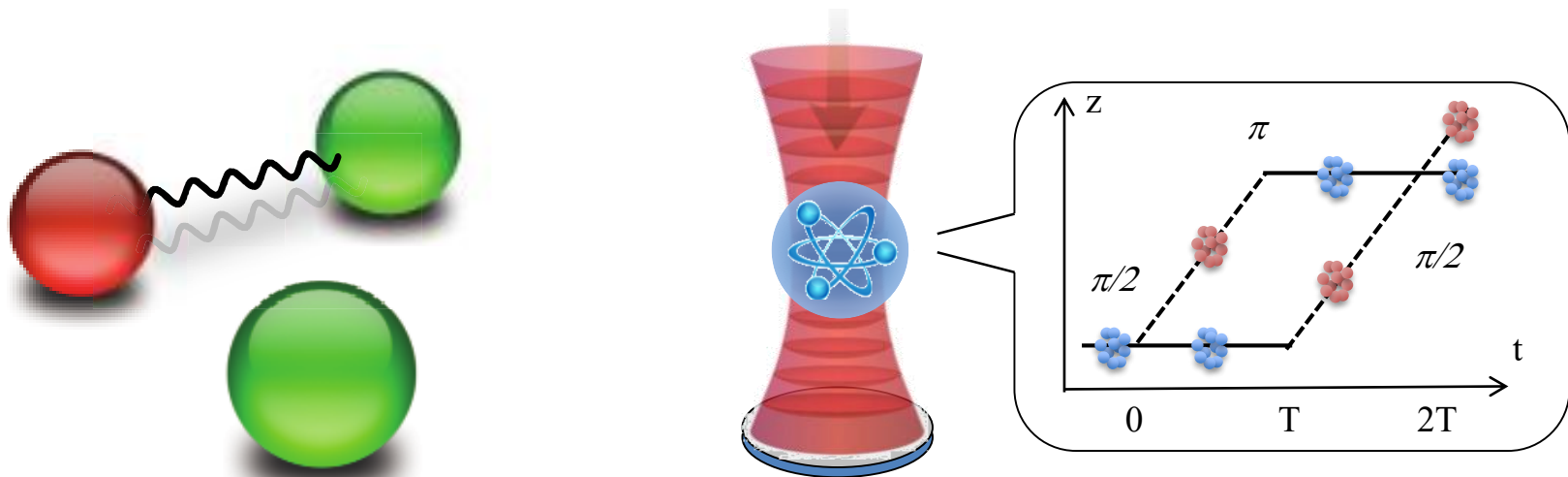
## Introduction

- Atom interferometers (AI) as inertial sensors and applications in space.

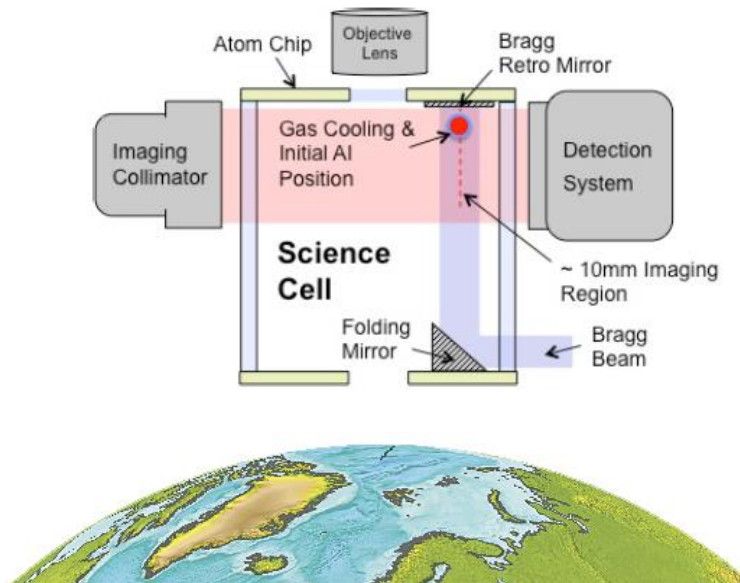
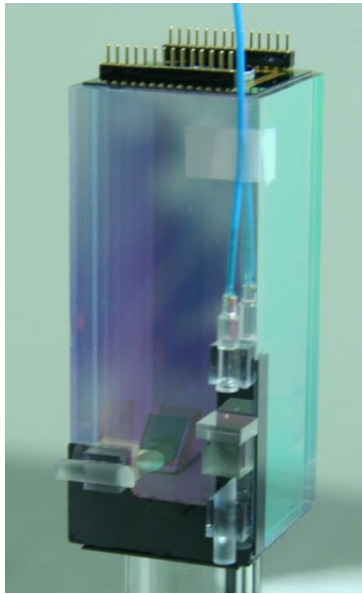
## Pathfinder studies with dual-species AI on the ISS

- Unprecedented atom-photon coherence time in CAL.
- Interferometric detection of relevant ISS vibration and rotation environment.
- Resonant molecular (Feshbach) physics in the ultracold regime for controlling systematics.
- Follow on studies and wish-list for BEcCAL.

## Strontium testbed at JPL to mature precision sensors/clocks for ground and space



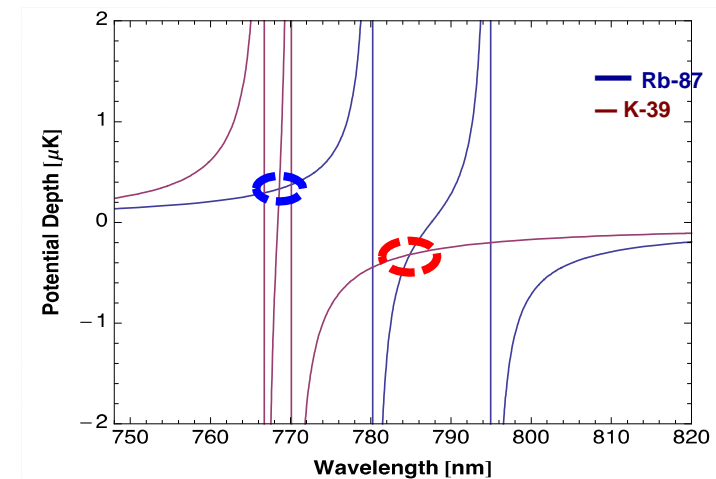
# Atom Interferometer Experiments Onboard the ISS



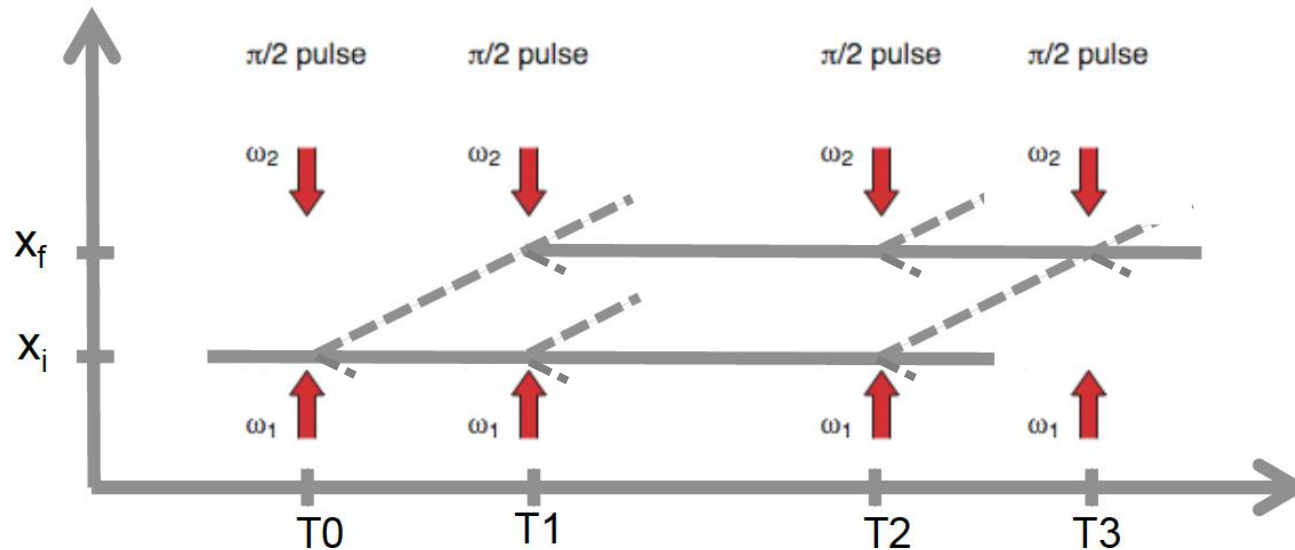
<b>Atom Numbers</b> ( <sup>87</sup> Rb and/or <sup>39</sup> K)	~10 <sup>4</sup> per species
<b>Cloud Temperature</b>	~ 100pK
<b>Free Expansion Time</b>	> 2s
<b>Bragg Beam Diameter</b>	> 0.75mm, < 1.4mm
<b>Bragg Wavelength</b>	785 nm
<b>Bragg Laser Power</b>	33mW in each frequency
<b>Frequency Components</b>	3 tunable & fully coherent
<b>Bragg Lattice Depth</b>	> 3 photon recoil energies
<b>AI Contrast (T = 0.5s)</b>	C > 25%

## Original Design for Pathfinder AI with CAL

- PI-recommended upgrade for EEP violation tests and space-technology advancement.
- Dual-species (<sup>39</sup>K-<sup>87</sup>Rb), simultaneous atom interferometer
- Bragg diffraction at the “magic” wavelength ( $\Omega_{\text{Rb}} = \Omega_{\text{K}}$ )
- Imaging detection for enhanced signal, reduced systematics
- Aligned with gravity for high sensitivity with quantum test masses in extended freefall.



## Spatially constrained AI

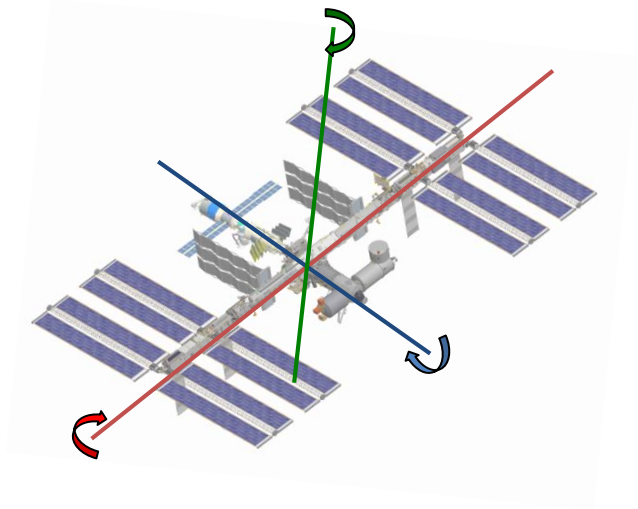
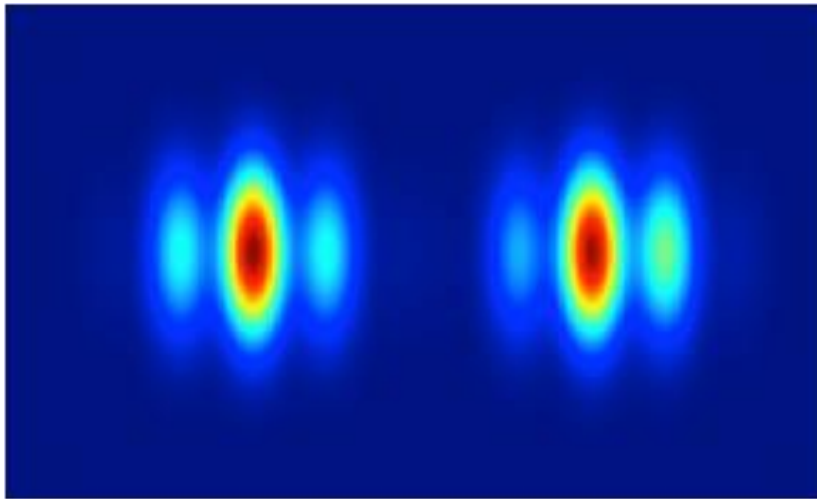


**Demonstrate AI atom-photon coherence beyond  $\sim 2$  seconds\* for  $^{87}\text{Rb}$ .**

- Constrained Bragg beam path length ( $\sim 2''$ ) and imaging region ( $\sim 10\text{mm}$ ) on CAL prohibit MZ AI with  $2T > 1.5$  s.
- Implement “spatially constrained AI” topology, limited by contrast and thermal expansion ( $\sim 100$  microns per second at 100 pK), sufficient for  $> 3\text{s}$  free fall.

\*Current record is  $2T = 2.3\text{s}$  by S. Dickerson *et al.*, “Multiaxis Inertial Sensing with Long-Time Point Source Atom Interferometry” PRL, **111**, 083001(2013)





## ISS rotation noise measurement from AI-induced phase fringes.

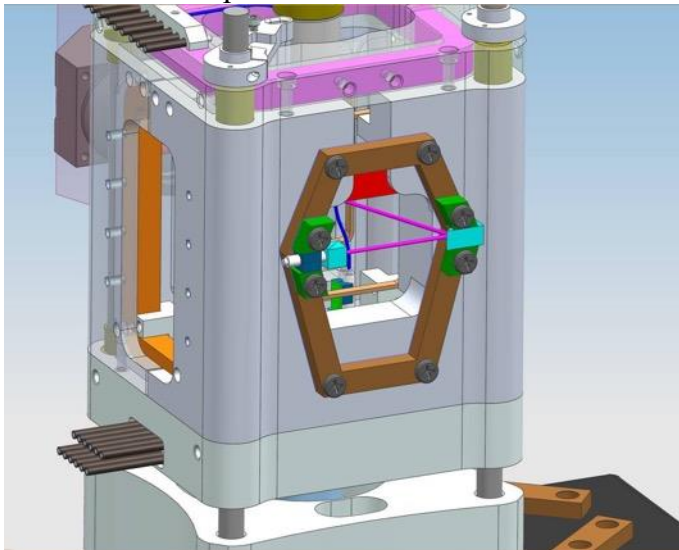
- For  $2T = 1\text{s}$ ,  $1\text{nK}$   $^{87}\text{Rb}$  cloud ( $\sigma_v$  is the thermal Gaussian width), and  $\Omega = \Omega_{\text{ISS}} = 2\pi/91\text{min}$ :

$$2k_{\text{eff}}(W \times S_v)T^2 = 3.6\text{rad}$$

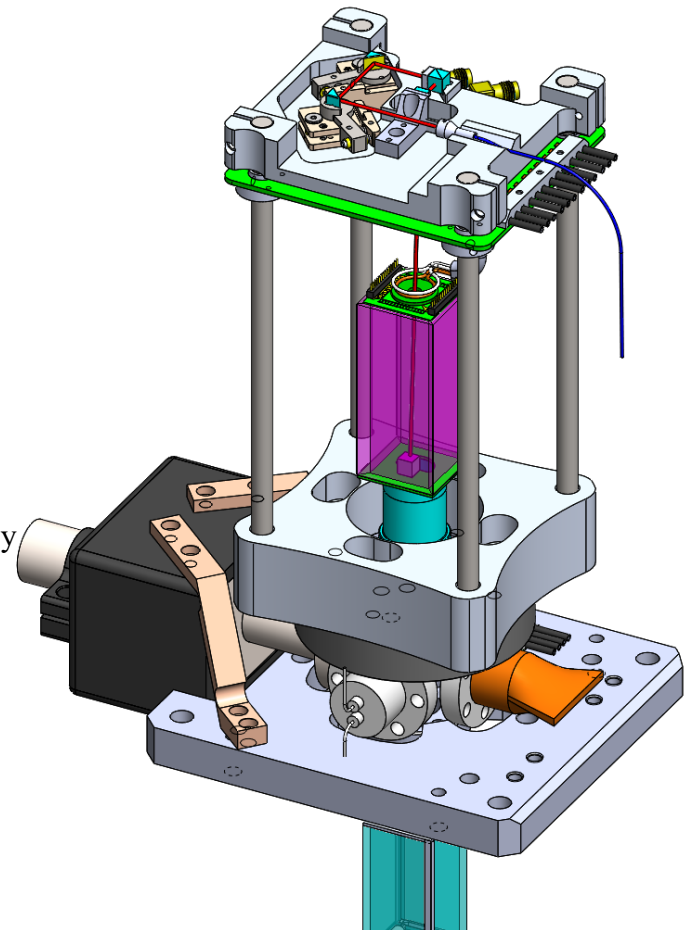
- Observation of fringes in each shot from rotation of CAL Physics Package on ISS.

## Trade study evaluated three design options:

- **Option I:** Horizontal interferometer beam
  - Lower risk, compatible with existing Physics Package designs.
  - Updated design to provide partial alignment along gravity vector (installation in overhead locker required).
- **Option II:** Vertical *through-window* interferometer beam.
  - New Physics Package for long-baseline interferometry.
  - Addresses lessons learned from JPL's CAL-1B Vacuum Failure Investigation.
  - Design concept presented in Final Report from ColdQuanta.
- **Option III:** Vertical offset interferometer beam (CAL-1B)
  - Interferometer beam is introduced at bottom of cell, and retro-reflected by on-chip mirror.



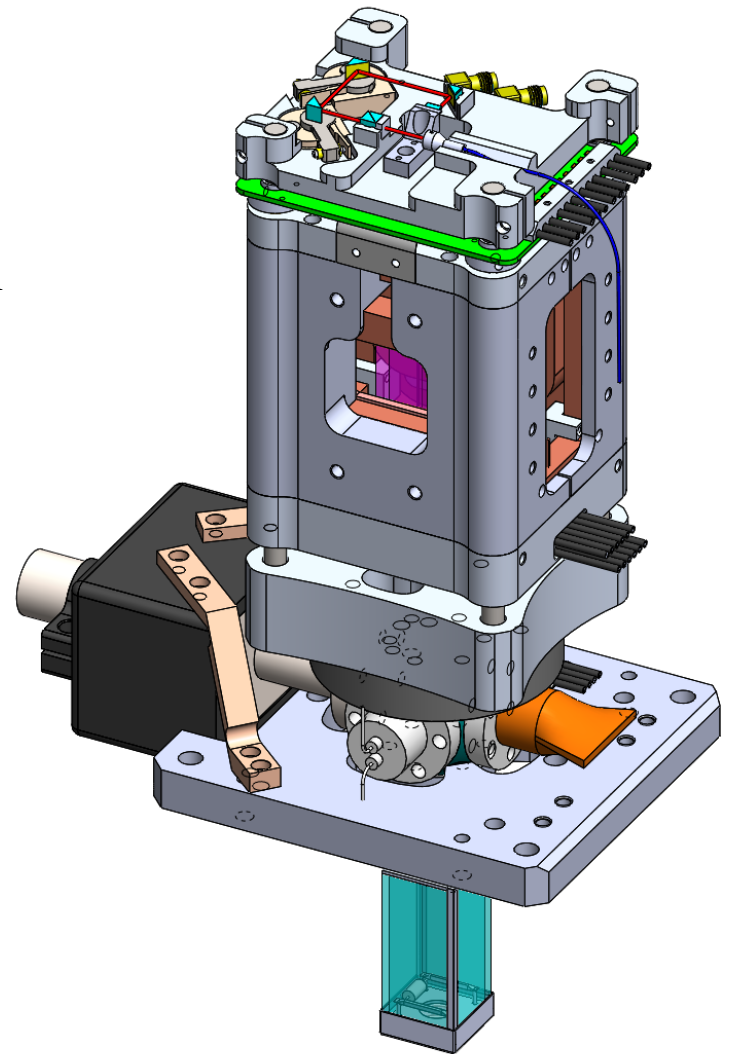
**Option I:** Horizontal beam geometry with beam delivery optics mounted to the MOT coil housing and beam aligned parallel to atom chip.



**Option II:** Long-baseline interferometer design concept with the AI beam transmitted through an on-chip window. Beam-steering optics are located on a separate platform above the atom chip.

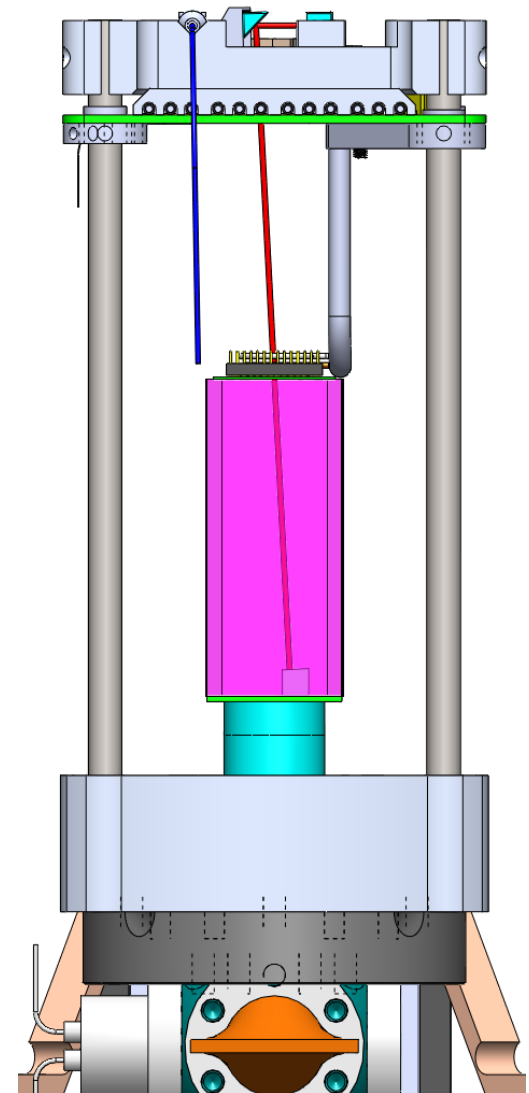
## Selected Design (Option II):

- ORU SM-3 Physics Package integrates the high-resolution objective with a new AI beam launching optic platform
  - Optical fiber is routed along same side as electrical connections to atom chip.
  - All other optical and mechanical interfaces are maintained.
- Atom chip window includes AR coatings on both surfaces to preserve beam quality.
- Physics Package includes a single in-vacuum retro-optic at bottom of UHV cell
  - Assembly is similar to the original CAL design, but eliminates two anodic bonds.
  - Offset retro-optic avoids interference with cold atom beam from 2D-MOT.
  - Slight ( $3^\circ$ ) angle of beam w.r.t. will be oriented along the “pitch” axis of the ISS to optimize alignment with gravity.



## Selected Design (Option II):

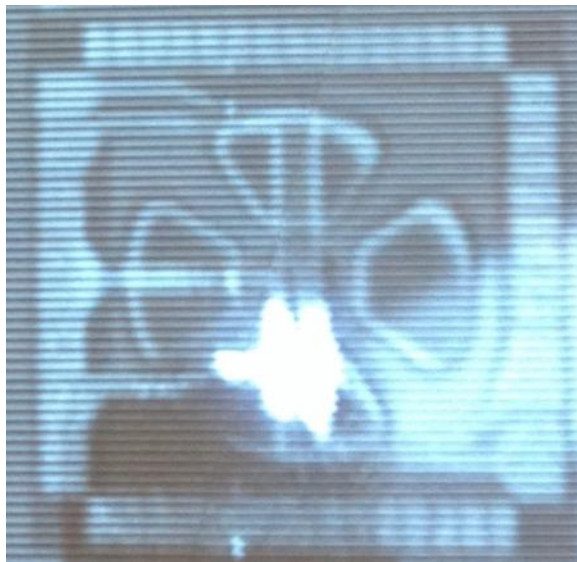
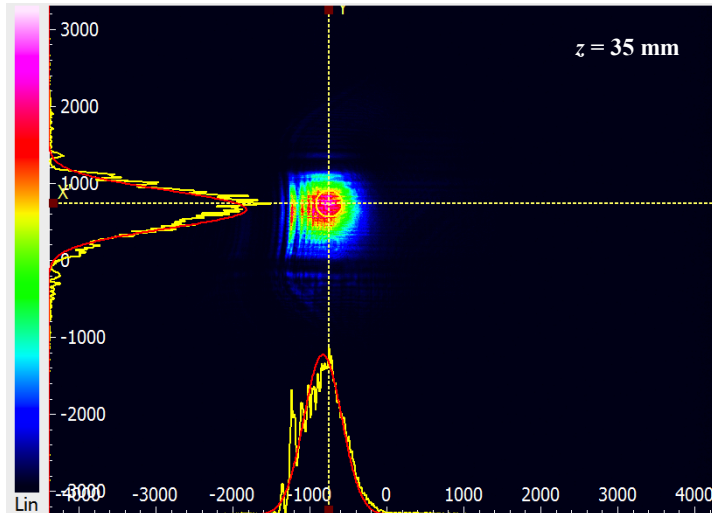
- ORU SM-3 Physics Package integrates the high-resolution objective with a new AI beam launching optic platform
  - Optical fiber is routed along same side as electrical connections to atom chip.
  - All other optical and mechanical interfaces are maintained.
- Atom chip window includes AR coatings on both surfaces to preserve beam quality.
- Physics Package includes a single in-vacuum retro-optic at bottom of UHV cell
  - Assembly is similar to the original CAL design, but eliminates two anodic bonds.
  - Offset retro-optic avoids interference with cold atom beam from 2D-MOT.
  - Slight ( $3^\circ$ ) angle of beam w.r.t. will be oriented along the “pitch” axis of the ISS to optimize alignment with gravity.





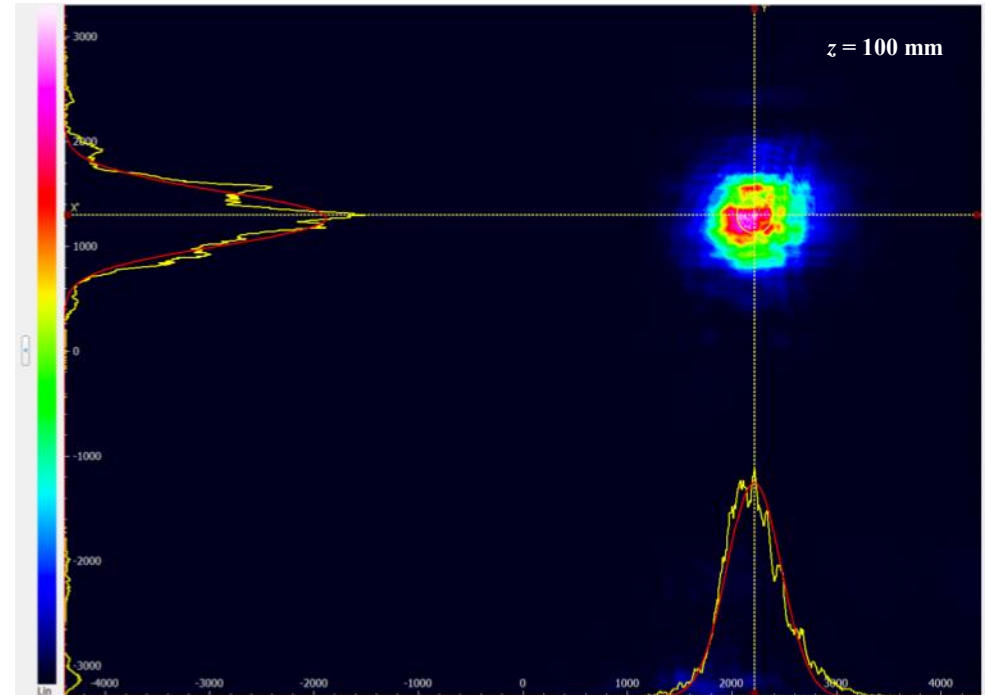
# Reflected Beam Quality

Reflected beam from sample atom chip ( $d_H = 1.4$  mm)



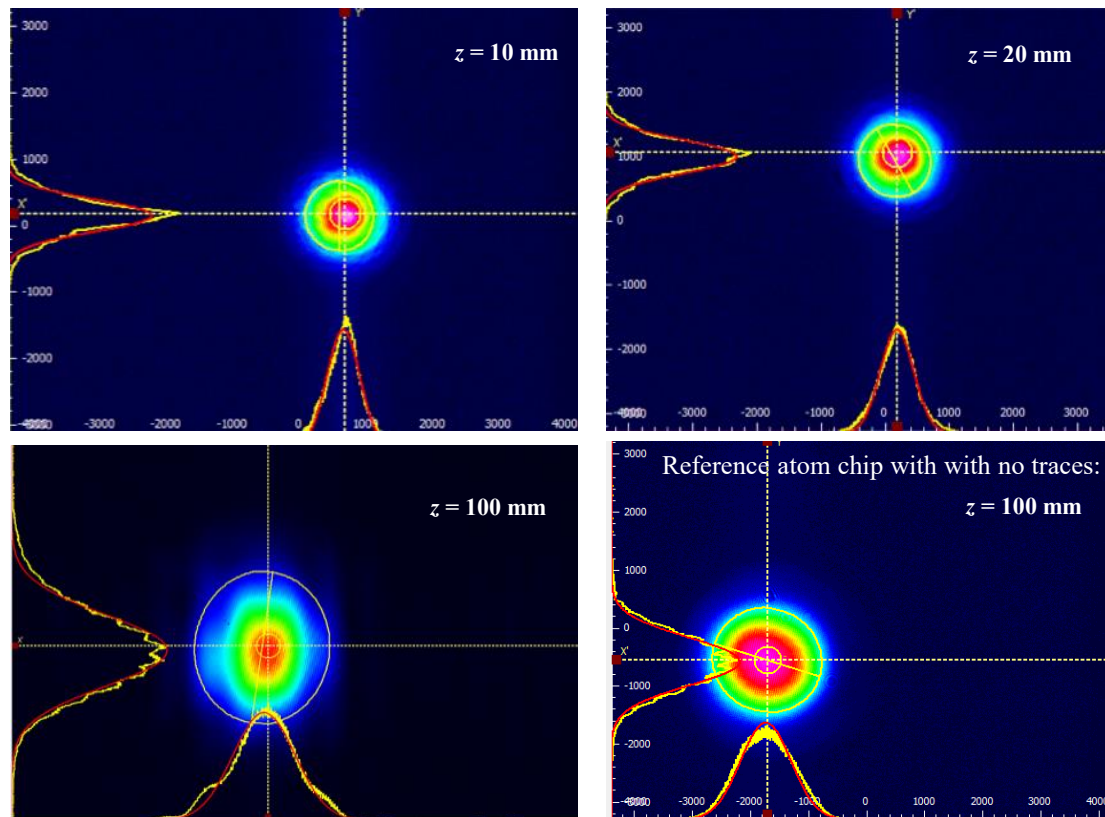
*Left:* Scattered light observed from sample atom chip

Reflected beam from CAL-1B atom chip ( $d_H = 1.4$  mm)



Measured beam profiles for reflected beam from sample atom chip (*left*) and CAL-1B (*right*). Observed significant diffraction and scattering from on-chip mirror due to  $H$ -wire traces.

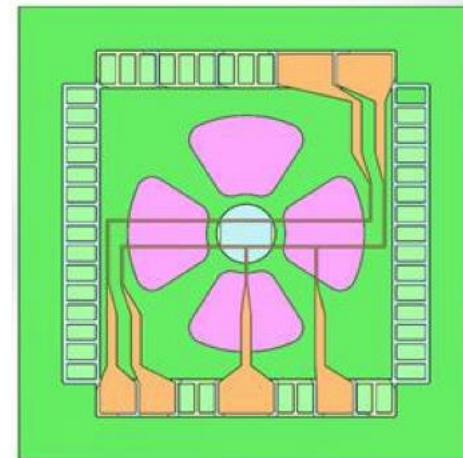
# Transmitted Beam Quality



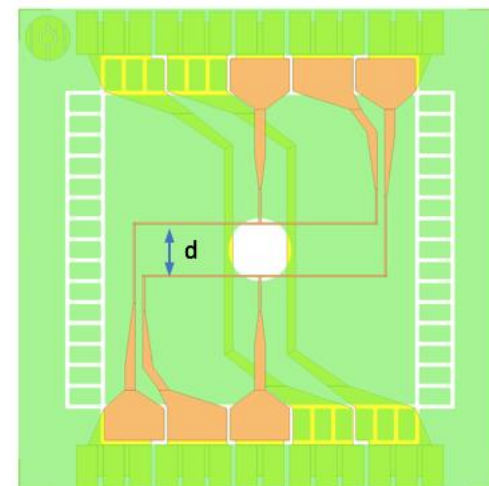
ColdQuanta measured beam profiles for a 1 mm diameter beam after transmission through an atom chip window with parallel  $H$ -wire traces with 1.4 mm separation

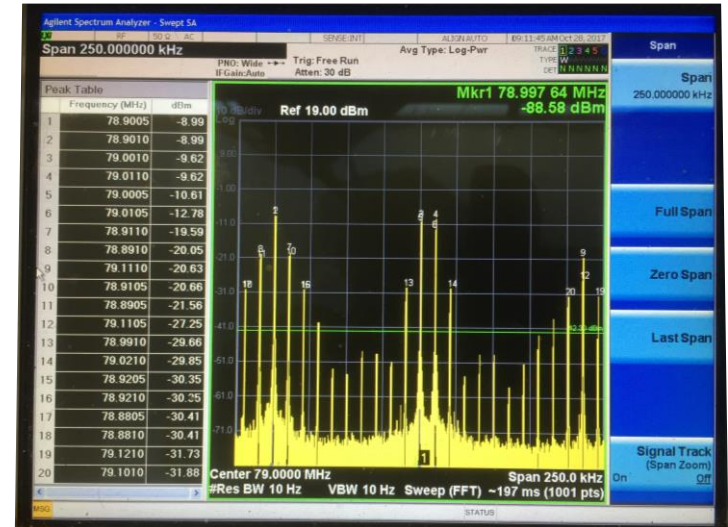
- Observed high spatial frequency fringes in far-field images ( $z = 100 \text{ mm}$ ), less noticeable in near-field, exploring maximum separation “ $d$ ” to mitigate.
- Minimal impact on trap depth, trap frequencies scale as  $d^{-1/2}$ .

Previous CAL AI chip design



Proposed Revision:





- Frequency and amplitude control via 80 MHz AOM driven by AWG amplified up-to 1 Watt.
- Light tuned to magic wavelength of 784.872nm, stable to better than +/- 250 MHz.
- 3 simultaneous frequency components, separated by tunable difference frequencies between 10 and 100 kHz for Bragg diffraction of Rb-87 and K-39.
- Frequency resolution better than 100Hz.
- Maximum 19.25 mW in each tone, giving lattice depth exceeding  $3 \cdot E_r$  for  $^{87}\text{Rb}$  in a 1mm diameter beam.
- Arbitrary pulse-shaping, with 10us time resolution. Amplitude of each tone individually controllable.
- Rise-fall times better than 10us.





Jose D'Incao



Dave Aveline

Ethan Elliott

## Special Thanks to:

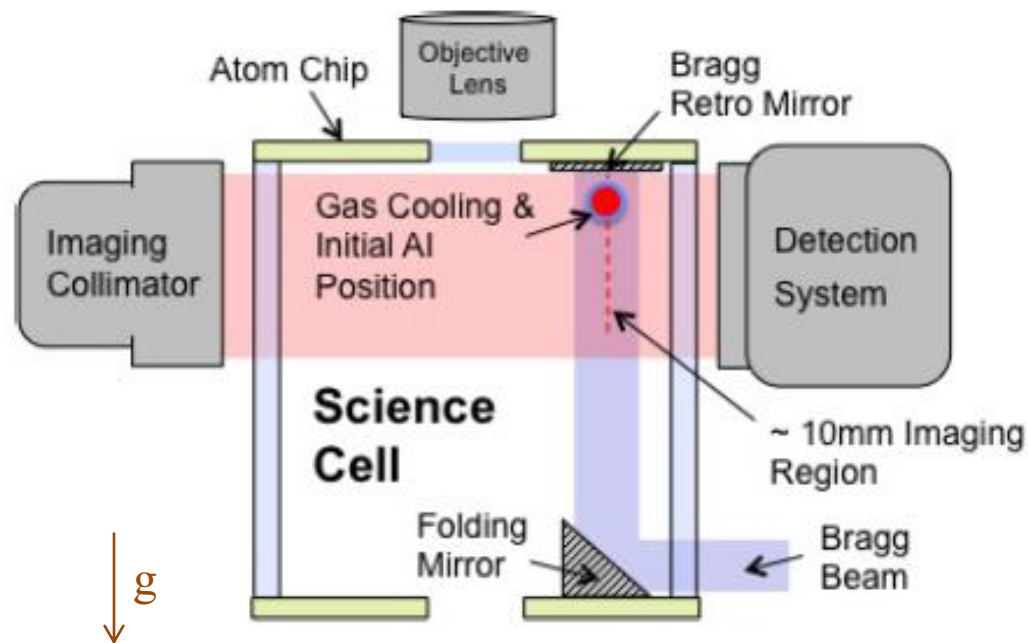
Robert Shotwell, Kamal Oudrhiri, Norm Lay, Rob Thompson, and the entire JPL team!

Mark Lee, Angel Otero, Diane Malarik, and all of our amazing support from SLPS/HEOMD and ISS PSO!

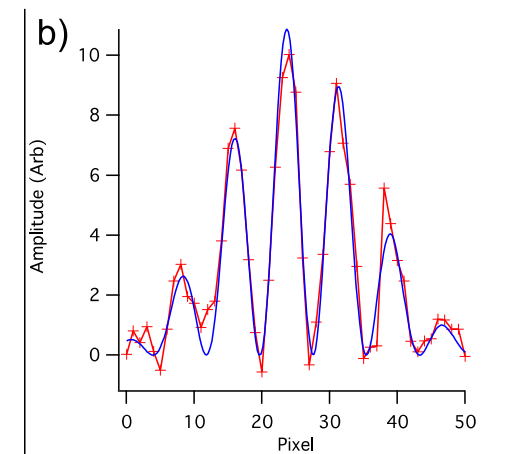
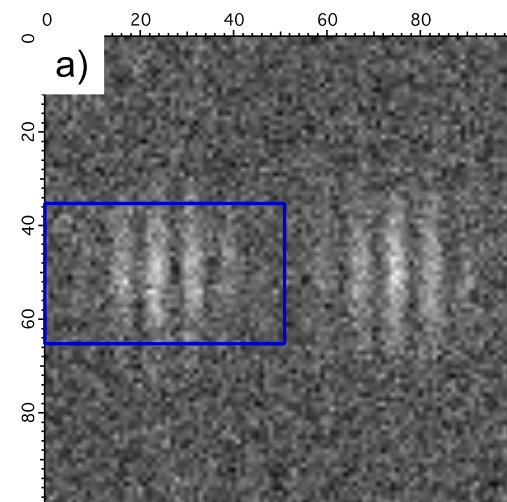


# Thank You.

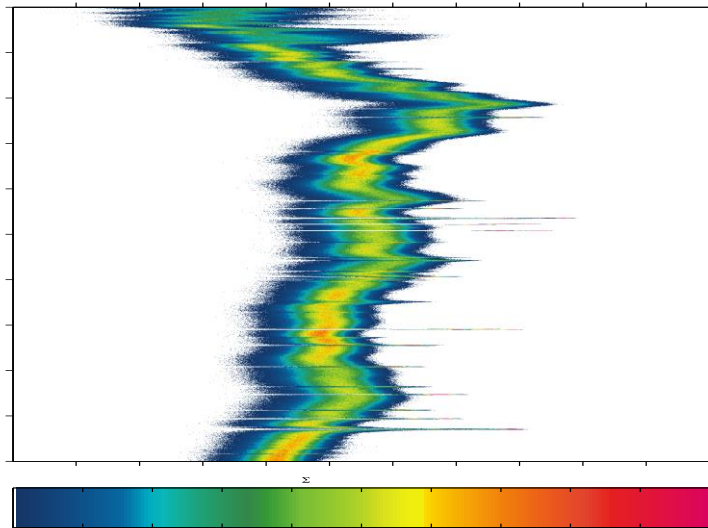
# ISS Rotation Noise Measurements



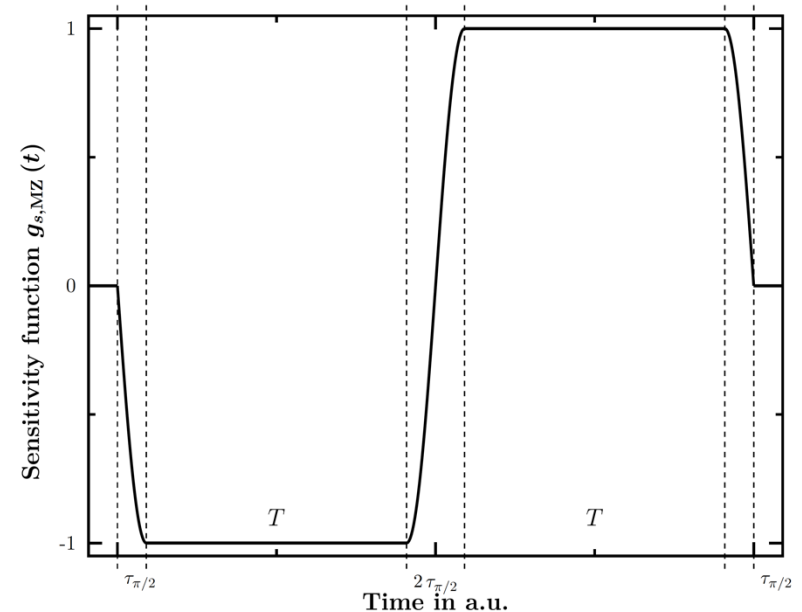
Velocity of station is into the page.  
 This is the ideal orientation for imaging fringes



(Top) Simulated fringe pattern on single-shot  $^{87}\text{Rb}$  2D density profile from DC angular velocity of the ISS with  $T = 0.5\text{s}$  AI and  $N_{87} = 10^5$ . (Bottom) Line profile after vertically averaging and fit (blue) to extract fringe spacing to a part in  $10^2$ .



Power spectral density of SAMS 121F04 three-axis sensor, exhibiting high sensitivity at 200Hz bandwidth [1]



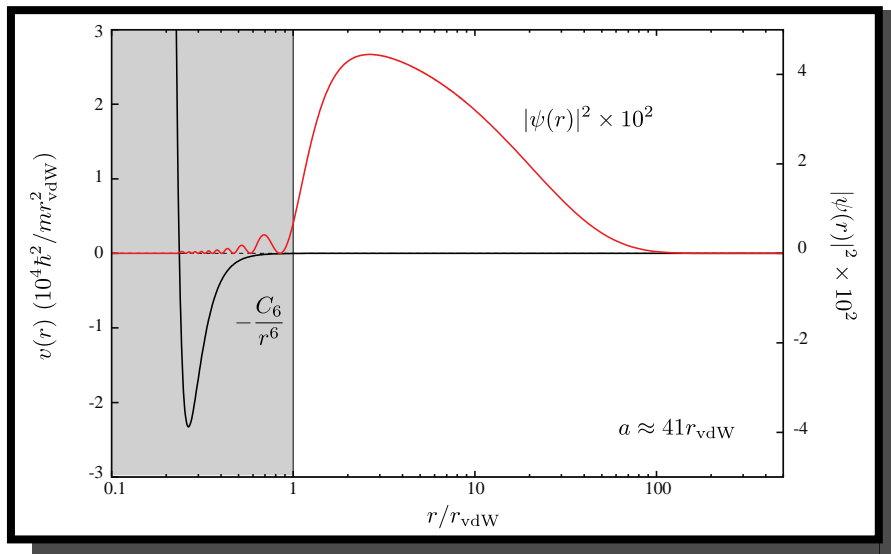
Sensitivity function for a Mach-Zehnder AI with pulse separation time  $T$  and pulse duration  $\tau_{\pi/2}$ . [2]

## Mach-Zehnder AI contrast is maximized for short pulse durations ( $t_{\pi/2}$ )

- Preferably  $t_{p/2} < 1\text{ms}$  to exceed thermal Doppler widths of sub-nanoKelvin clouds and broadening from known ISS vibration noise.
- SAMS and MAMS sensors onboard the ISS have bandwidth  $< 500\text{ Hz}$ .
- Important to measure ISS vibration noise with AI for relevant noise characterization.

1. Principal Investigator Microgravity Services (PIMS) website: [pims.grc.nasa.gov](http://pims.grc.nasa.gov)
2. Figure from D. Schlippert *Quantum Tests of the Universality of Free Fall*, PhD thesis, Leibniz Universität, Hannover (2014)

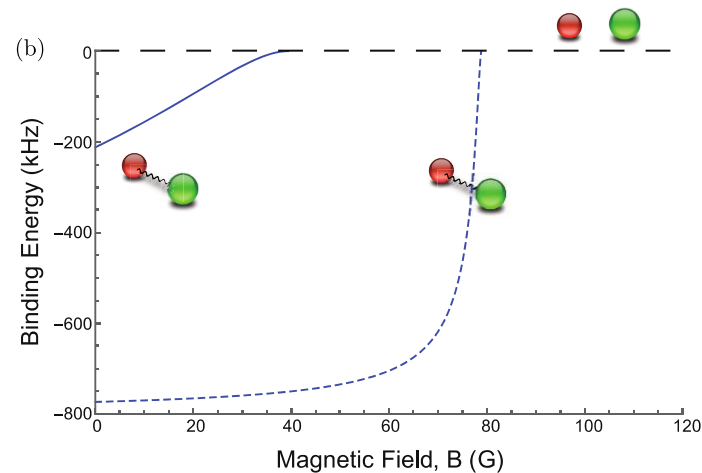
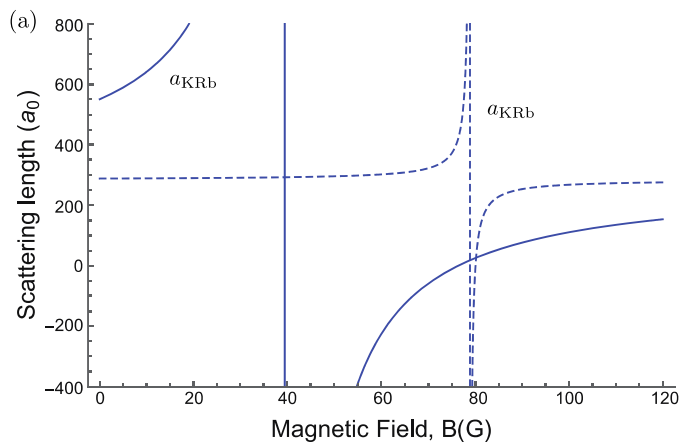
## Universality



Dimer Size:  $\langle r \rangle = a / 2$

Binding Energy:  $E_D \approx \frac{-\hbar^2}{ma^2}$

$^{41}\text{K} - ^{87}\text{Rb}$



## Enhanced association and dissociation of heteronuclear Feshbach molecules in a microgravity environment

J. P. D’Incao,<sup>1,2</sup> M. Krutzik,<sup>3,4</sup> E. Elliott,<sup>4</sup> and J. R. Williams<sup>4</sup>

<sup>1</sup>*JILA, University of Colorado and NIST, Boulder, Colorado, USA*

<sup>2</sup>*Department of Physics, University of Colorado, Boulder, Colorado, USA*

<sup>3</sup>*Humboldt-Universität zu Berlin, Institut für Physik, Berlin, Germany*

<sup>4</sup>*Jet Propulsion Laboratory, California Institute of Technology, CA, USA*

We study the association and dissociation dynamics of weakly bound heteronuclear Feshbach molecules using transverse RF-fields for expected parameters accessible through the microgravity environment of NASA’s Cold Atom Laboratory (CAL) aboard the International Space Station, including sub nanoKelvin temperatures and atomic densities as low as  $10^8/\text{cm}^3$ . We show that under such conditions, thermal and loss effects can be greatly suppressed resulting in high efficiency in both association and dissociation of Feshbach molecules with mean size exceeding  $10^4 a_0$ , and allowing for the coherence in atom-molecule transitions to be clearly observable. Our theoretical model for heteronuclear mixtures includes thermal, loss, and density effects in a simple and conceptually clear manner. We derive the temperature, density and scattering length regimes of  $^{41}\text{K}$ - $^{87}\text{Rb}$  that allow optimal association/dissociation efficiency with minimal heating and loss to guide upcoming experiments with ultracold atomic gases in space.

PACS numbers: 34.50.-s, 34.50.Cx, 67.85.-d, 67.85.-d

## Microgravity provides a unique regime for Feshbach Physics

- Unearthly low energy scales.
- No gravitational sag.
- Extended timescales for few-body physics and loss.

## Studies available in BEcCAL include

- Few-body (e.g. Efimov and Halo-molecule) physics.
- Source preparation (e.g. well-overlapped or nearly-degenerate dual-species gases).
- Precision measurements for fundamental physics.



# Wish List for BEcCAL

- $^{85}\text{Rb}$  sympathetically cooled with  $^{87}\text{Rb}$  to near-degeneracy.
- Feshbach fields up-to 300 Gauss with capabilities for field-modulation with bandwidth  $> 1$  kHz.
- Al Bragg beam at the magic wavelength for  $^{85}\text{Rb}$ - $^{87}\text{Rb}$  (780nm  $\pm$  20 GHz) and with diameter  $> 5$  cm to accommodate long-time Al in microgravity.
- Near-simultaneous, dual-species imaging along 2 axes perpendicular to Al wave vector for cloud-overlap and fringe detection.
- Magnetic field shielding or active suppression to below 1 mGauss and 1 mGauss/cm over Al region.